Available online at www.sciencedirect.com

ScienceDirect

Journal of the European Ceramic Society 30 (2010) 3103–3109

www.elsevier.com/locate/jeurceramsoc

# Thermal properties of homogenous lanthanum hexaaluminate/alumina composite ceramics

Zahra Negahdari[a,*], Monika Willert-Porada[a], Florian Scherm[b]

[a] *Materials Processing, University of Bayreuth, 95440 Bayreuth, Germany*
[b] *Metals and Alloys, University of Bayreuth, 95440 Bayreuth, Germany*

Received 15 January 2010; received in revised form 4 July 2010; accepted 16 July 2010

## Abstract

Lanthanum hexaaluminate has the potential to be applied in thermal barrier coatings due to its relative low thermal conductivity and low sinterability at temperatures higher than 1100 °C. One of the main problems in developing this material as a thermal barrier coating is difficulty in controlling the microstructure in order to combine the low thermal conductivity with high structural reliability.

The idea behind this study was to take advantage simultaneously of the low thermal conductivity of lanthanum hexaaluminate and of the high mechanical properties of alumina by developing alumina-rich and lanthanum hexaaluminate-rich alumina/lanthanum hexaaluminate ceramic composites. The thermal properties of the alumina/hexaaluminate ceramic composites were compared as a function of temperature and lanthanum hexaaluminate content (20–80 vol.%). The results showed that the alumina/lanthanum hexaaluminate ceramic composites have sufficient low thermal conductivity to be used in thermal barrier coatings.

*Keywords:* B. Composites; C. Thermal properties; C. Thermal conductivity; D. $Al_2O_3$; Lanthanum hexaaluminate ($LaAl_{11}O_{18}$)

## 1. Introduction

Thermal barrier coatings (TBCs) are generally composed of a porous, insulating ceramic oxide top layer (yttria-stabilized zirconia (YSZ) is state of the art) which provides thermal protection, a thermally grown aluminum-rich oxide layer (TGO) which provides oxidation and hot corrosion protection, and an underlying aluminide (nickel or platinum) bond layer which is used to form the TGO layer.[1,2] For integration into the TBCs, materials require low thermal conductivity, a sufficiently high thermal expansion coefficient, phase stability up to temperatures higher than 1400 °C, stable pore morphology, and chemical and mechanical compatibility with the underlying layers. Lower thermal conductivity, high thermal durability, and improved lifetime while considering the overall cost are still demanded in TBCs development. The increase in thermal conductivity of coatings caused by densification due to increasing the operating temperature is an additional important issue which reveals the need for materials with low sinterability at elevated temperatures. These materials should substitute YSZ for long-term high temperature applications due to the common problems with YSZ (e.g., dramatic aging at temperatures above 1100 °C and post-sintering, which reduce the thermal conductivity). Since oxygen diffusivity of zirconia increases with temperature and leads to constant oxidation of the bond layer and consequently failure of the TBCs in operation, materials with lower oxygen diffusivity are required as well.[1,3]

Lanthanum hexaaluminate, abbreviated as LHA, with a defective magnetoplumbite crystal structure and a plate-like grain structure have the potential to be applied as high temperature TBCs. Although the thermal conductivity of LHA (0.8–2.6 $W m^{-1} K^{-1}$) is to some extent higher than that of YSZ (0.6–2.3 $W m^{-1} K^{-1}$), however its low Young's modulus, low sinterability, superior structural and thermochemical stability up to 1400 °C, stable pore structure, lower oxygen diffusivity, and phase compatibility with $Al_2O_3$ as the TGO layer up to 1800 °C draw attentions to investigate LHA as a candidate for high temperature TBCs.[4–6] The low thermal conductivity of

---

* Corresponding author. Tel.: +49 921 557207; fax: +49 921 557205.
*E-mail address:* zahra.negahdari@uni-bayreuth.de (Z. Negahdari).

0955-2219/$ – see front matter © 2010 Elsevier Ltd. All rights reserved.
doi:10.1016/j.jeurceramsoc.2010.07.026

LHA ceramics top layers is due to the defects and porosity which they introduce into the system. Poor intrinsic mechanical properties of LHA in addition to the presence of porosity could limit the structural reliability and fracture toughness of LHA-based TBCs. Our previous study showed that addition of alumina to the lanthanum hexaaluminate ceramics enhances their mechanical properties.[7] Alumina/LHA composite ceramics with different LHA content and engineered chemical composition and porosity which can be applied as a single homogenous layer or as multilayer systems to provide good mechanical properties and low thermal conductivities are introduced and studied in this paper as a new generation of the TBCs. These materials in a multilayer TBC system can provide alumina-rich inner layers with low porosity and good mechanical properties compatible with a TGO layer and porous LHA-rich outer layers capable of prolonged higher temperature exposure.[8] Thermal properties of the alumina/LHA composite ceramics as a function of LHA content and temperature are compared in this paper toward better understanding of application of LHA-based ceramics in the TBCs. Although materials for TBCs were the aim of this study, classical ceramic processing was applied because of the necessity to tailor the microstructure in a wide range of LHA volume fraction.

## 2. Experimental procedure

Alumina and alumina/LHA ceramics with the variation of in situ formed LHA content from 20 to 80 vol.% were prepared as discussed elsewhere.[9] For in situ formation of LHA in the composite ceramics, samples were sintered by two-stage sintering in air (1675 °C/10 min–1500 °C/2 h).

Density and porosity of the samples were measured by the method based on Archimedes' principle. In addition, open pore-size distribution of the sintered samples was measured with a Micromeritics, Autopore III mercury porosimeter. A field emission gun scanning electron microscope LEO 1530 (FEG-SEM, Gemini) was used for microstructural characterization.

Thermal diffusivity measurement of the samples was made by means of the laser flash technique (LFA 427, Netzsch GmbH) for slab samples (10 mm × 10 mm × 3 mm) in argon atmosphere.[10,11] Because the alumina/LHA composites are semi-transparent to near infrared wavelengths, the samples were coated with a thin graphite layer in order to avoid the propagation of the laser radiation through the thickness of the material. This also improves the laser beam absorption and the emitted signal of the back face. Thermal diffusivity was measured over the temperature range RT–1100 °C with a temperature interval of 100 °C and three measurements at each temperature.

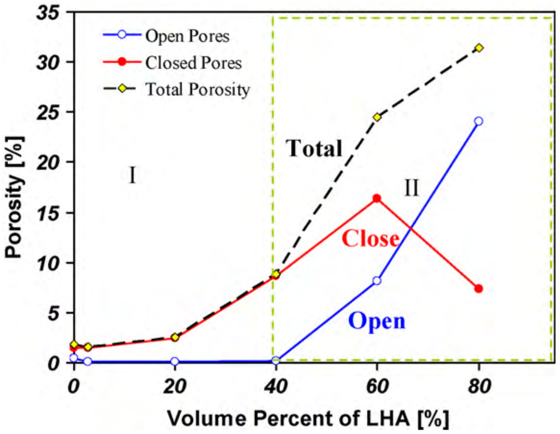

Fig. 1. Volume fraction of open and closed pores of the alumina/LHA composite ceramics as a function of LHA content.

Thermal conductivity, $\lambda$, of the samples was obtained using Eq. (1)

$$\lambda = \alpha \rho c_p \qquad (1)$$

where $\alpha$ is the thermal diffusivity, $\rho$ is the density and $c_p$ is the specific heat of the composite ceramics.[12]

## 3. Results

The density and porosity of the alumina and alumina/LHA composite ceramics after sintering are tabulated in Table 1 as a function of the in situ formed LHA content. Due to the in situ formation of LHA platelets with low sinterability, densification was retarded and porosity of composites was increased by increasing LHA content. The porosity and the volume of the open pores and closed pores of the alumina and alumina/LHA composites are represented in Fig. 1. The pore-size distribution of these composites is illustrated in Fig. 2, as well. An increase in the porosity, the volume fraction of open pores, and the average pore size is observed with increasing in the LHA content. The volume fraction of closed pores was increased with the increase in LHA content up to 60 vol.% and decreased with further LHA addition.

For better understanding of the thermal properties of the alumina/LHA composite ceramics, the microstructures of the sintered alumina and LHA/containing composite ceramics are compared as a function of LHA content in Fig. 3. LHA platelets are the lighter phase in BSE mode because of the content of the heavy element lanthanum. Increase in volume fraction of

Table 1
Relative density and porosity of sintered alumina/LHA composite ceramics.

| | Lanthanum hexaaluminate content (vol.%) | | | | |
|---|---|---|---|---|---|
| | 0 | 20 | 40 | 60 | 80 |
| Density (g/cm$^3$) | 3.91 | 3.917 | 3.7 | 3.093 | 2.836 |
| Relative density (TD %) | 98 | 97 | 91 | 75 | 68 |
| Porosity (%) | 2 | 3 | 9 | 25 | 32 |

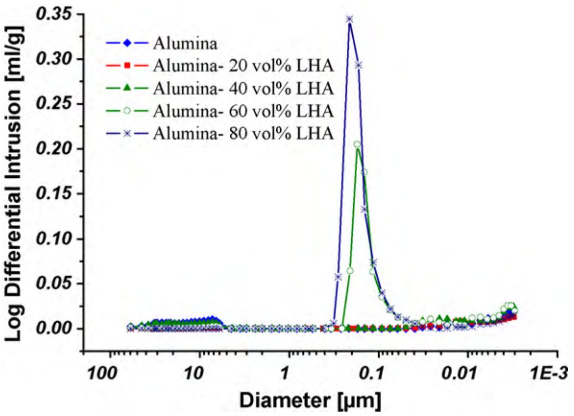

Fig. 2. Comparison of pore-size distribution for alumina and alumina/LHA composite ceramics as a function of LHA content.

the LHA platelets and reduction in grain size of alumina grains with dark contrast is observed by the increase of LHA content.

Measured thermal diffusivity data for the alumina and alumina/LHA composite ceramics as a function of temperature and LHA content are exhibited in Fig. 4.

For calculating thermal conductivity of the composites according to Eq. (1), the measured densities listed in Table 1 were used and the specific heats were calculated for each composition using the Neumann–Kopp rule (Eq. (2)).

$$c(T) = \sum_{n=1}^{n} f_i c_i(T) \tag{2}$$

where $f_i$ is the mass fraction of each phase and $c_i(T)$ is the corresponding specific heat for the constituents $Al_2O_3$ and $LaAl_{11}O_{18}$.[13] The heat capacities of alumina and LHA were taken from the literature.[14,15]

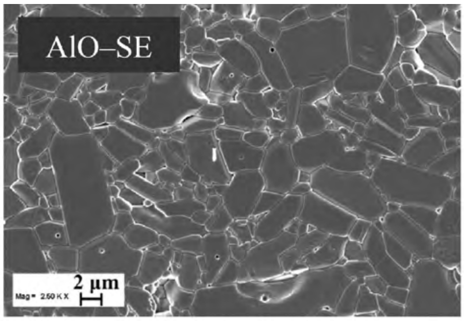

(a) alumina

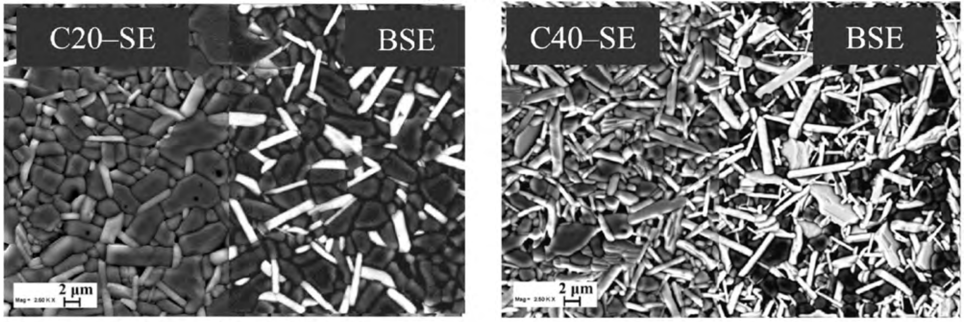

(b) alumina/20 vol.% LHA (c) alumina/40 vol.% LHA

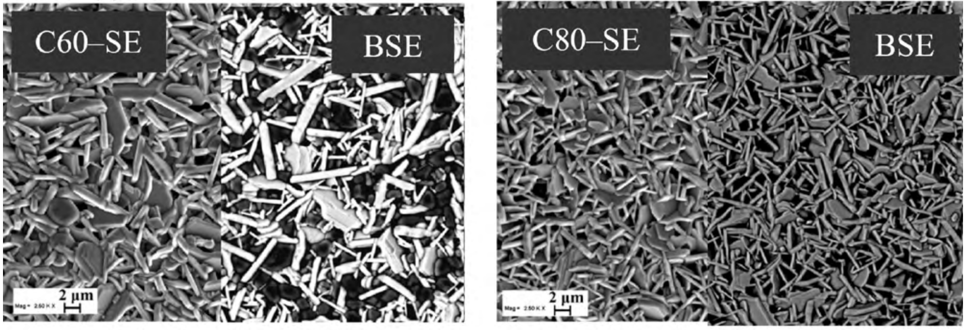

(d) alumina/60 vol.% LHA (e) alumina/80 vol.% LHA

Fig. 3. Secondary (SE) and backscattered (BSE) FE-SEM micrographs of microstructures obtained for alumina and $Al_2O_3$/LHA composite ceramics after sintering at 1675 °C/10 min–1500 °C/2 h.

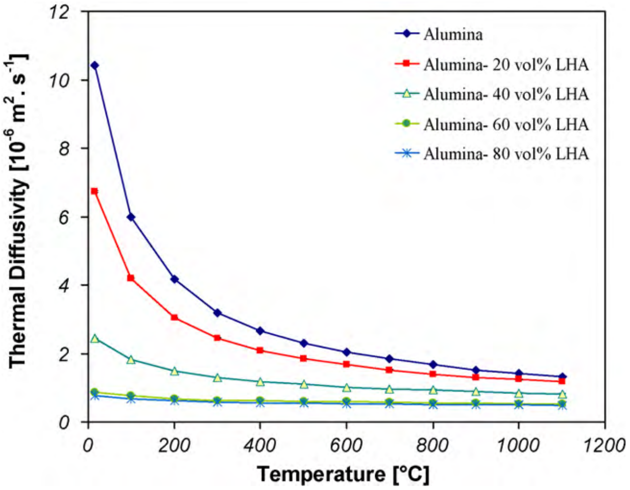

Fig. 4. Thermal diffusivity of monolithic alumina and alumina/LHA composite ceramics as a function of temperature.

To calculate the effective heat capacity per unit volume $(\rho c)_{\text{eff}}$, the following simple approximation was used:

$$(\rho c)_{\text{eff}} = (\rho c)_{\text{comp}}(1-\varphi) + (\rho c)_{\text{air}}\varphi \tag{3}$$

where $\varphi$ is the volume fraction of porosity in the samples, $\rho_{\text{comp}}$, and $\rho_{\text{air}}$ are the densities of the porosity-free composites and air, respectively, and $c_{\text{comp}}$ and $c_{\text{air}}$ are the corresponding heat capacities.[16] The calculated heat capacity and thermal conductivity of the alumina and alumina/LHA composites are plotted in Figs. 5 and 6, respectively. A clear trend is apparent for the measured thermal diffusivity, calculated thermal conductivity, and heat capacity as a function of the LHA content: they decrease with increasing volume fraction of LHA. As illustrated in Figs. 4 and 6, the thermal diffusivity and conductivity of the pure alumina and alumina/LHA composite ceramics decrease at elevated temperatures when compared with low temperature values, although the heat capacity increases with increasing temperature.

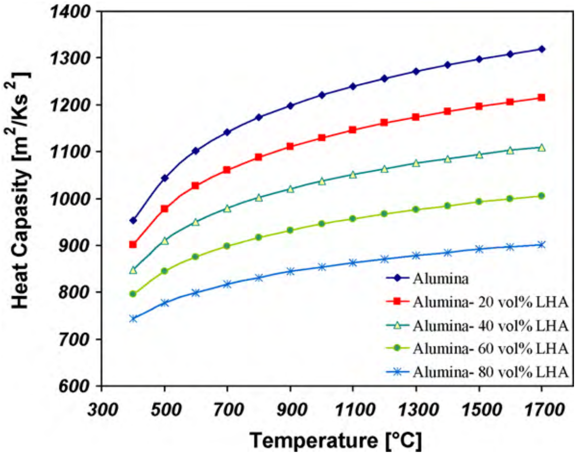

Fig. 5. Calculated specific heat capacity of alumina and alumina/LHA composite ceramics.

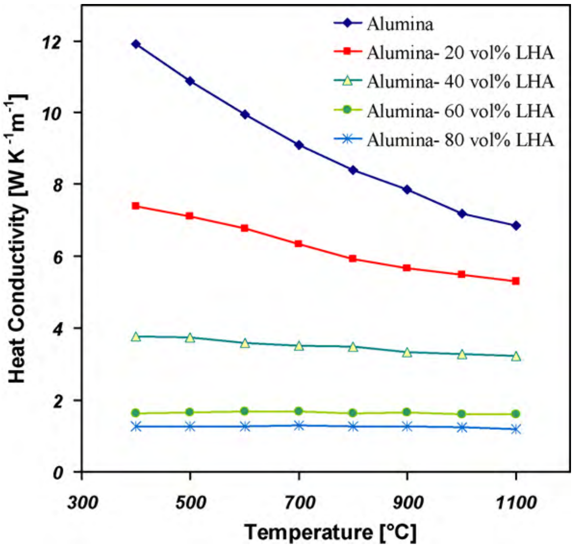

Fig. 6. Thermal conductivity of alumina and alumina/LHA composite ceramics.

## 4. Discussion

### 4.1. Thermal properties of monophase and polyphase ceramics

Temperature-dependent behavior of the thermal diffusivity depends upon the microstructure and the mechanisms of heat conduction operating at elevated temperature.

Heat transfer in ceramics can proceed by different mechanisms: convection, conduction, and radiation. The convective thermal conductivity is negligible in the alumina/LHA composite ceramics due to the pore size less than 1 mm. Phonons are responsible for the heat transfer at low temperature by conduction. The heat conductivity mechanism varies dependent of temperature. Photon conductivity, which means heat transport by radiation, often becomes the significant factor for thermal conductivity in ceramics at high temperatures (>1000 °C) whereas phonon conductivity is the dominant mechanism at low temperatures.

Since based on the shape of the diffusivity–temperature curves, radiative transport seems unlikely, the phonon conductivity is discussed in the following analysis of the influence of temperature and LHA amount on the thermal conductivity of the alumina/LHA composite ceramics.

From the kinetic theory of phonons in solids, the thermal conductivity, $\lambda$, of an insulating solid is expressed as:

$$\lambda = \frac{1}{3} c\upsilon l \tag{4}$$

where $c$ is the heat capacity per unit volume, $\upsilon$ is the velocity of vibrational propagation, and $l$ is the conductive mean free path.[17]

For the pure alumina, the thermal conductivity decreases from 13 $\text{WK}^{-1}\,\text{m}^{-1}$ to 8 $\text{WK}^{-1}\,\text{m}^{-1}$ over the temperature range of 25–1100 °C. It is observed that the thermal conductivities of the alumina/LHA composite ceramics are lower than that of the pure alumina at lower temperatures, but at higher temperatures that difference slightly decreases. The shape of the thermal conductivity curves obtained for the alumina and $Al_2O_3$/LHA composite ceramics matches a phonon conduction mechanism up to 1000 °C which is limited by intrinsic phonon scattering as $1/T$. Phonon–phonon interactions, which are important over a wide temperature range, are the dominant process for thermal resistivity for low defect crystals.[17] When the temperature elevates to a sufficiently high level, the mean free path decreases to a value near the lattice spacing, and the conductivity is expected to be independent of temperature. At this temperature level various lattice imperfections (defects, grain boundaries, and impurities), second phase precipitates or particles with low conductivity (e.g., the LHA grains), and the porosity can further enhance phonon scattering and significantly decrease the effective conductive mean free path through the sample, therefore reduce the conductivity. In ceramic composites containing less than 20 vol.% LHA (i.e., LHA a minor phase dispersed in alumina as continuous major phase), the heat conduction is dominated by the alumina phase. Above about 40 vol.% LHA, the LHA phase is continuous with dispersed alumina grains and also porosity. Therefore the heat conductivity of the LHA phase is predominant. In comparison with alumina, LHA ceramics with defective non-stoichiometric complex structures have a greater tendency toward thermal scattering of phonons and consequently exhibit a lower thermal conductivity coefficient.[18] Therefore one of the main reasons for temperature-independent behavior of the thermal conductivity for composites with higher concentrations of LHA (60–80%) is the presence of defects. The magnitude of the phonon mean free path reduction increases with the concentration of point defects, LHA content.

In addition to the intrinsic point defects of LHA, linear defects (i.e., grain boundaries) can also act as scattering sites and decrease the phonon conductivity. This reduction can be enhanced by decreasing the average grain size. Smith et al.[19] discuss grain-boundary thermal resistance and also consider following equation for expressing how it affects the thermal conductivity of the polycrystalline solid.

$$\frac{1}{\lambda_{\text{poly}}} = \frac{1}{\lambda_{\text{crystal}}} + nR_{\text{int}} \tag{5}$$

where $\lambda_{\text{poly}}$ is the thermal conductivity of the polycrystalline material, $\lambda_{\text{crystal}}$ is the thermal conductivity of the single crystal, $n$ is the number of interfaces per unit length, and $R_{\text{int}}$ is the thermal resistance of a grain-boundary plane.[19] Literature suggests that a typical value of the grain-boundary thermal resistance is in the range $10^{-8}$–$10^{-7}$ m$^2$ K W$^{-1}$.[19] However, it is not expected that all materials yield identical values. In any case, comparing the FE-SEM micrographs of the monolithic alumina with 20 and 40 vol.% alumina/LHA composite ceramics (Fig. 3) by decreasing the grain size via increase in the LHA content, there is a strong increase in the length of grain boundaries crossed by the heat flowing through the solid phase. In polycrystalline materials with fine grain size, such as the above composites, where the phonon mean free path is not much smaller than the grain size, the influence of the grain boundary is not negligible. Therefore, by increasing the LHA content from 20 to 40%, the total thermal resistance is increased. At higher temperatures the influence of grain boundaries is negligible, because the mean free path is much smaller than the grain size.

### 4.2. Thermal properties of porous composite ceramics

In addition to phonon–phonon scattering and presence of LHA and defects, porosity influences the thermal conductivity of the alumina/LHA composite ceramics as well. Pores as structural discontinuities reduce thermal conductivity, but for high-density materials, it is not a significant factor. The conduction decreases also due to the tortuous solid concentration path and the presence of a low conductivity gas in the mesopores (Knudsen effect). The hindering effect of phonon-pore scattering (due to the reflection from solid-pore interfaces) is significant for small pore size. The measured density of the pure alumina and alumina/LHA composite ceramics (Table 1) decreased from 98 to 68% while the LHA content increased. Concurrently, the total porosity, open pores volume percentage, and the average pore size increased. The degradation of the thermal diffusivity and conductivity can additionally be attributed to the increase in porosity. The difference in the pore size dominates the slope of thermal conductivity decrease as a function of temperature and LHA content.

As indicated in Fig. 2, the pore-size distribution of composites with less than 60 vol.% LHA reveals an increase of average pore size from approximately 2 to 20 nm with increasing LHA content. Such small mesopores will not be detected as open pores by the Archimedes density measurement, used to measure the density; rather they are considered as “closed porosity” (Fig. 1). The volume of mesopores increases up to 9 vol.% in the alumina/40 vol.% LHA composite ceramic with an average pore size of ∼20 nm. By increasing the LHA content from 40 to 60, the total porosity increases to 25 vol.%. The bimodal pore-size distribution and the closed/open-pore volume ratio of alumina/60 vol.% LHA composite imply on increase in the volume fraction of mesopores with a mean pore size of ∼20 nm as well as the amount of macropores with mean pore size of ∼150 nm. Thus, a high proportion of the pores of alumina/60 vol.% LHA is of very small dimension. In the alumina/80 vol.% LHA composite a tremendous decrease in the volume of mesopores is observed; notwithstanding the volume of macropores with a mean pore size of ∼200 nm increases. In 60 vol.% LHA the transition from the closed-pore region I to the percolated-pore region II is approached at 25% of porosity (Fig. 1).

The thermal diffusivity and conductivity decreased by adding LHA up to 40 vol.% into the system due to phonon-pore scattering. In composite ceramics with 20–60 vol.% LHA, the influence of the pore size (presence of mesopores) on the thermal conductivity of gases due to the Knudsen effect should also be studied.

The gaseous thermal conductivity of pores in materials is frequently expressed as:

$$\lambda_{\text{gas}} = \frac{\lambda^0_{\text{gas}}}{1 + \alpha Kn} \tag{6}$$

where $\lambda^0_{\text{gas}}$ is the thermal conductivity in free air, $Kn$ is the Knudsen number, and $\alpha$ is a constant specific to the gas in the pores.[20] Flow regimes of gas molecules are classified by the Knudsen number; for $Kn \geq 1$ it is called Knudsen flow and gas molecules hardly collide with each other in this regime, but mainly come into collision with the pore wall. For $Kn \leq 1$ it is called viscous flow, and gas molecules flow like a liquid, so that collisions between gas molecules are very frequent. $Kn$ is expressed as $l_{\text{mfp}}$, the mean free path of a gas molecule over $l_{\text{cl}}$, the characteristic length.

$$Kn = \frac{l_{\text{mfp}}}{l_{\text{cl}}} \tag{7}$$

In general $l_{\text{cl}}$ is interpreted as the average pore size in porous materials. Two kinds of gases are supposed to be in pores: argon from the measurement atmosphere and air because of the sintering atmosphere. Since the mean free paths of air and argon gas molecules are less than 100 nm, it was presumed that for the porous materials, the Knudsen flow participated considerably in degradation of the thermal conductivity of the alumina/60 vol.% LHA containing approximately 17% mesoporosity. The Knudsen effect does not significantly influence the thermal properties of alumina/80 vol.% LHA with an average pore size of 200 nm and where the percolation of pores is reached.

At the end of this part, two facts should be mentioned. One is that in spite of the authors' interest, modelling the thermal diffusivity or the conductivity of these composites by different models (e.g., effective medium theory) is not possible since they have so many variables that they cannot be measured. There are at least five separate parameters that affect the diffusivity of these materials: (i) volume fraction of hexaaluminate, (ii) volume fraction of porosity, (iii) orientation of the hexaaluminate plates, (iv) orientation of porosity (spherical, aligned along the platelets, etc), and (v) unknown thermal diffusivity anisotropy of the hexaaluminate phase. Then there may be contact resistance effects between the two phases. No effective medium theory is likely to reproduce these observations without detailed knowledge of these parameters. The only possible way to compare results with theory is to use some finite-element-based method in which the actual microstructures are digitized and the heat transfer equations are solved.

The second is that the microstructure of these materials due to the processing procedure is completely different to those in TBCs. TBCs are deposited by different methods like thermal spraying (TS) and electron beam-physical vapour deposition (EB-PVD). The EB-PVD deposited top coats have columnar microstructures consist of vertical pores oriented perpendicular to the surface whereas horizontal pores oriented parallel to the coating surface are observed in thermal sprayed coatings.[21,22] And as discussed the coating thermal conductivity is strongly dependent on the pore morphology and porosity. Thus, microstructural anisotropy (orientation and morphology) and higher porosity results in anisotropic and lower thermal conductivity. The microstructures of alumina/LHA composites developed in this work have rounded or ribbon-shaped pores with the average pore size smaller than 200 nm. This pore size is smaller than the size of interlamellar pores (0.1–3 μm) in TBCs. Despite the slight orientation in pores and LHA platelets in these composites, no distinguishable preferential orientation is observed in the microstructures of these composites as compared with those of TBCs deposited by thermal spraying and EP-CVD. Although different thermal properties are expected for alumina/LHA TBCs prepared by common coating processes, thermal conductivity of alumina coatings decreases with increase in the LHA content.

## 5. Conclusions

Thermal properties of lanthanum hexaaluminate/alumina composite ceramics were studied as a function of temperature and LHA content (20–80 vol.%). The thermal diffusivity and the thermal conductivity of the composite ceramics decreased with increasing temperature and LHA volume fraction. Phonon conductivity was considered as the main heat transfer mechanism in the temperature range that the thermal properties of the composites were investigated. For better understanding of the thermal properties, microstructural observations and porosity measurements were included. Phonon scattering by phonon and defective LHA structure, grain boundaries, and pores were assumed to have contributed to the degradation of the thermal properties of the composites.

## Acknowledgment

Sincere thanks are extended to Mr. P. Kostolansky and Mrs. M. Gietl for their great contributions in sample preparation and editing the text respectively. The financial support of the Bavarian Science Foundation within the doctoral grant DPA-52/05 is gratefully acknowledged.

## References

1. Clarke DR, Levi CG. Material design for the next generation of thermal barrier coating. *Annu Rev Mater Res* 2003;**33**:383–417.
2. Evans AG, Clarke DR, Levi CG. The influence of oxides on the performance of advanced gas turbines. *J Eur Ceram Soc* 2008;**28**:1405–19.
3. Azzopardi A, Mevrel R, Ramond BS, Olson E, Stiller K. Influence of aging on structure and thermal conductivity of Y-PSZ and Y-FSZ EB-PVD coatings. *Surf Coat Technol* 2004;**177–178**:131–9.
4. Friedrich C, Gadow R, Schirmer T. Lanthanum hexaluminate: a new material for atmospheric plasma spraying of advanced thermal barrier coatings. *J Therm Spray Technol* 2001;**10**(4):592–8.
5. Gadow R, Lischka M. Lanthanum hexaluminate: novel thermal barrier coatings for gas turbine applications: materials and process development. *Surf Coat Technol* 2002;**151–152**:392–9.
6. Cinibulk MK. Thermal stability of some hexaluminates at 1400 °C. *J Mater Sci Lett* 1995;**14**:651–4.
7. Negahdari Z, Willert-Porada M, Pfeiffer C. Mechanical properties of dense to porous alumina/lanthanum hexaaluminate composite ceramics. *Mater Sci Eng A* 2010;**527**(12):3005–9.
8. Negahdari Z, Willert-Porada M. Microstructure tailored functionally graded alumina/lanthanum hexaaluminate ceramics for application as thermal barrier coatings. *Adv Eng Mater* 2009;**11**(12):1034–8.
9. Negahdari Z, Willert-Porada M. Tailoring the microstructure of reaction-sintered alumina/lanthanum hexaaluminate particulate composites. *J Eur Ceram Soc* 2010;**30**(6):1381–9.

10. Shinzato K, Baba T. A laser flash apparatus for thermal diffusivity and specific heat capacity measurements. *J Therm Anal Calorim* 2001;**64**(1):413–22.
11. Parker WJ, Jenkins RJ, Butler CP, Abbott GL. Flash method of determining thermal diffusivity, heat capacity, and thermal conductivity. *J Appl Phys* 1961;**32**(9):1679–84.
12. Vozár L, Hohenauer W. Uncertainty of thermal diffusivity measurements using the laser flash method. *Int J Thermophys* 2005;**26**(6):1899–915.
13. Swalin RA. *Thermodynamics of solids*. New York: John Wiley; 1962.
14. Touloukian YS, Buyco FH. *Thermophysical properties of matter, the TPRC data series vol. 5, specific heat: nonmetallic solids*. New York, Washington: IFI/Plenum; 1970.
15. Wu P, Pelton AD. Coupled thermodynamic/phase diagram assessment of the rare earth oxide–aluminum oxide binary systems. *J Alloys Compd* 1992;**179**(1–2):259–87.
16. Sun J. Evaluation of ceramic matrix composites by thermal diffusivity imaging. *Int J Appl Ceram Technol* 2007;**4**(1):75–87.
17. Kingery WD, Bowen HK, Uhlmann DR. *Introduction to ceramics*. 2nd ed. New York: John Wiley and Sons; 1976.
18. Park JG, Cormack AN. Defect structures and nonstoichiometry in lanthanum hexa-aluminate. *J Eur Ceram Soc* 1999;**19**:2249–56.
19. Smith DS, Fayette S, Grandjean S, Martin C, Telle R, Tonnessen T. Thermal resistance of grain boundaries in alumina ceramics and refractories. *J Am Ceram Soc* 2003;**86**(1):105–11.
20. Lee OJ, Lee KH, Yim TJ, Kim SY, Yoo KP. Determination of mesopore size of aerogels from thermal conductivity measurements. *J Non-Cryst Solids* 2002;**298**:287–92.
21. Garcia E, Miranzo P, Soltani R, Coyle TW. Microstructure and thermal behavior of thermal barrier coatings. *J Therm Spray Technol* 2008;**17**(4):478–85.
22. Flores Renteria A, Saruhan B, Schulz U, Raetzer-Scheibe H-J, Haug J, Wiedenmann A. Effect of morphology on thermal conductivity of EB-PVD PYSZ TBCs. *Surf Coat Technol* 2006;**201**:2611–20.